Available online at www.sciencedirect.com

ScienceDirect

Journal of the European Ceramic Society 34 (2014) 1209–1217

www.elsevier.com/locate/jeurceramsoc

Effect of grain size on the energy storage properties of $(Ba_{0.4}Sr_{0.6})TiO_3$ paraelectric ceramics

Zhe Song [a], Hanxing Liu [a,*], Shujun Zhang [b], Zhijian Wang [a], Yatong Shi [a], Hua Hao [a], Minghe Cao [a], Zhonghua Yao [a], Zhiyong Yu [a]

[a] *State Key Laboratory of Advanced Technology for Materials Synthesis and Processing, Wuhan University of Technology, Wuhan 430070, Hubei, PR China*
[b] *Materials Research Institute, Pennsylvania State University, University Park, PA 16802, USA*

Received 19 September 2013; received in revised form 24 November 2013; accepted 26 November 2013
Available online 18 December 2013

Abstract

$(Ba_{0.4}Sr_{0.6})TiO_3$ (BST) ceramics with various grain sizes (0.5–5.6 μm) were prepared by conventional solid state reaction methods. The effect of grain size on the energy storage properties of BST ceramics ($T_c \approx -65\,^{\circ}C$) was investigated. With decreasing grain sizes, a clear tendency toward the diffuse phase transition was observed and the dielectric nonlinearity was reduced gradually, which can be explained by the Devonshire's phenomenological theory (from the viewpoint of intrinsic polarization). Based on the multi-polarization mechanism model, the relationship between the polarization behavior of polar nano-regions (the extrinsic nonlinear polarization mechanisms) and grain size was studied. The variation of the grain boundary density was thought to play an important role on the improvement of dielectric breakdown strength, account for the enhanced energy density, which was confirmed by the complex impedance spectroscopy analysis based on a double-layered dielectric model.

Keywords: Paraelectric BST; Grain size; Dielectric nonlinearity; Energy storage property; The grain boundary density

1. Introduction

Recently, $(Ba_{1-x}Sr_x)TiO_3$ ($x = 0$–1) (BST) has received considerable attentions due to the potential applications in the field of electric energy storage, by the virtue of their high power density and good reliability.[1] The Curie point (T_c) of $(Ba_{1-x}Sr_x)TiO_3$ can be controlled by varying the mole fraction of Sr, accompanied by significant variation of dielectric properties, which can be tailored for specific applications.[2]

With the continuous miniaturization of components, size-dependent properties have been of great interest in many types of electronic ceramics including BST. Grain size effects on the phase evolution, microstructure and dielectric properties of $BaTiO_3$-based ceramics have been reported since 1950s.[3–5] Previous reports on the properties of BST ceramics for the potential energy storage applications showed a strong dependent on the grain sizes, where the large variation of dielectric constant,[6] the decrease of dielectric nonlinearity[7] as well as the improvement of dielectric breakdown strength[8] were confirmed to be associated with the refinement of grain size.

Based on the observation of grain size effect in $BaTiO_3$-based ceramics, many mechanisms have been proposed, such as internal stress,[4] 90° ferroelectric domains[5] and the role of grain boundary layer,[9] etc. However, most of the publications about the grain size effect and its intrinsic mechanisms were focused on materials with ferroelectric phase,[10,11] other than paraelectric phase, which was considered more potential for electric energy storage dielectrics.[12] So it is interesting to discuss the grain size effect for BST ceramics with paraelectric phase, to improve the energy storage performance by the refinement of grain sizes and establish the relationship between specific intrinsic mechanisms (such as the grain boundary density, other than the role of ferroelectric domains) and the macroscopic properties.

In this study, $(Ba_{0.4}Sr_{0.6})TiO_3$ was chosen as the research object, which show paraelectric phase structure at room temperature ($T_c \approx -65\,^{\circ}C$) and relatively low dielectric loss ($tg\,\delta \approx 0.005$), moderate dielectric constant (~1000), and high dielectric breakdown strength (~150 kV/cm) as well as good dielectric stability under dc bias field,[13] being potential for electric energy storage applications.[14] Following these

* Corresponding author. Tel.: +86 27 87653330; fax: +86 27 87885813.
E-mail address: lhxhp@whut.edu.cn (H. Liu).

0955-2219/$ – see front matter © 2013 Elsevier Ltd. All rights reserved.
http://dx.doi.org/10.1016/j.jeurceramsoc.2013.11.039

considerations, a comprehensive study of the grain size effect on the energy storage properties of $(Ba_{0.4}Sr_{0.6})TiO_3$ with paraelectric phase and its corresponding mechanisms were investigated.

2. Experimental

The $(Ba_{0.4}Sr_{0.6})TiO_3$ polycrystalline ceramics were prepared by the conventional solid state reaction method with high purity (99.95%) commercial powders of $BaCO_3$, $SrCO_3$ and TiO_2. The stoichiometric mixtures were ball milled with zirconium media in ethanol for 24 h. After drying, the powders were calcined at 1180 °C for 4 h in air and then pressed to form disk-shaped samples at 150 MPa. To prepare dense ceramics with various grain sizes, the green pellets were sintered at different temperatures (1260–1400 °C) for 2 h. Finally, the sintered ceramics were polished to 0.3 mm in thickness and coated with fire-on silver electrodes for electrical measurements.

Density measurement was carried out using the Archimedes method. XRD analysis was performed on the sintered pellets using Cu K_α radiation (X'Pert PRO, PANalytical, Holland). Microstructure and grain size were observed on thermally etched surface of the sintered samples by field-emission scanning electron microscope (FE-SEM) (S-4800, Hitachi, Japan). Average grain sizes of BST were statistically calculated by using Image Pro plus software, which were simulated by the average length of diameters passing through objects' centroid, measured at 2 degree intervals.

The dielectric nonlinearity was measured by a precision impedance analyzer (Agilent 4980 A, Agilent, USA) connected with a dc power supply. The dielectric breakdown strength and *P–E* hysteresis loop were examined at room temperature using a Radiant precision workstation (Radiant RT66A) based on the Sawyer-Tower circuit at 10 Hz. The energy storage density γ was evaluated by integrating the area between the polarization axis and the discharge curve in the *P–E* hysteresis loop, which is given by the following equation:

$$\gamma = \int_0^{E_b} E\ dP \tag{1}$$

where P and E are the polarization and the electric field, E_b is the breakdown electric field.[15]

3. Results and discussion

3.1. Phase characterization and microstructure observation

XRD patterns of the BST ceramics with different sintering temperatures are shown in Fig. 1. The phase structure was found to maintain the same at different sintering temperatures, where no obvious second phase was observed. For all samples, the split of (2 0 0) peaks corresponding to the tetragonality was not observed, revealing that all samples exhibit paraelectric phase with cubic perovskite structure.

Fig. 2 shows the FE-SEM images of BST ceramics with various grain sizes obtained at different sintering temperatures. For better observation, the sintered samples were polished about 300 μm off and then thermal etched 100 °C below their

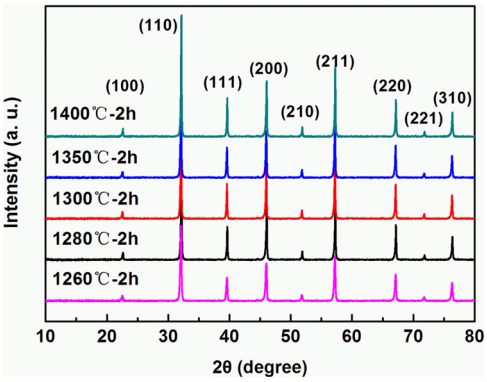

Fig. 1. XRD patterns of BST ceramics under different sintering conditions.

respective sintering temperatures. As observed in the figures, all samples show uniform and homogeneous morphologies, while the grain size was found to strongly depend on the sintering temperature. After the calculation on SEM images by Image Pro Plus software, it was found that with increasing sintering temperatures from 1260 °C to 1400 °C, the average grain size changed from 0.5 μm to 5.6 μm, which can be regarded as an ideal range at micro scale to illustrate the grain size dependent properties effectively.[5]

Fig. 3 gives the measured densities for the sintered samples, which were found to be above 96% of the theoretical value, regardless the sintering temperature. In this case, the variation of densities has minimal impact on the properties of BST with different grain sizes,[16] thus the change of grain size is considered as the dominant factor affecting the macroscopic properties.

The temperature-dependent dielectric properties for BST ceramics with different grain sizes are given in Fig. 4, which were measured at 10 kHz frequency. For all the samples, the dielectric constants are about 1500 with dielectric losses being less than 0.005 at room temperature, the Curie temperatures (T_c) were found to locate at around −65 °C, indicating the room temperature paraelectric phase, which is in good agreement with the XRD results (shown in Fig. 1). As the grain size reduced from 5.6 μm to 0.5 μm, a significant decrease of dielectric constant around the Curie temperature was observed, with a clear tendency toward a diffuse phase transition, which was thought to be inherently associated with the internal stress between grains.[17,18]

3.2. Grain size effect on the dielectric nonlinearity and the nonlinearity mechanisms

The dielectric nonlinearity represents the nonlinear decrease of the dielectric constant as a function of applied voltage, which will not benefit the energy storage density. It has long been recognized that this decrease of dielectric constant with electric field is an intrinsic property of ferroelectric ceramics, while for ceramics with paraelectric phase, the nonlinearity is much lower.[19]

3.2.1. Grain size effect on the dielectric nonlinearity

Fig. 5 exhibits the field dependence of the dielectric constants at 10 kHz for BST ceramics, with the external dc bias field

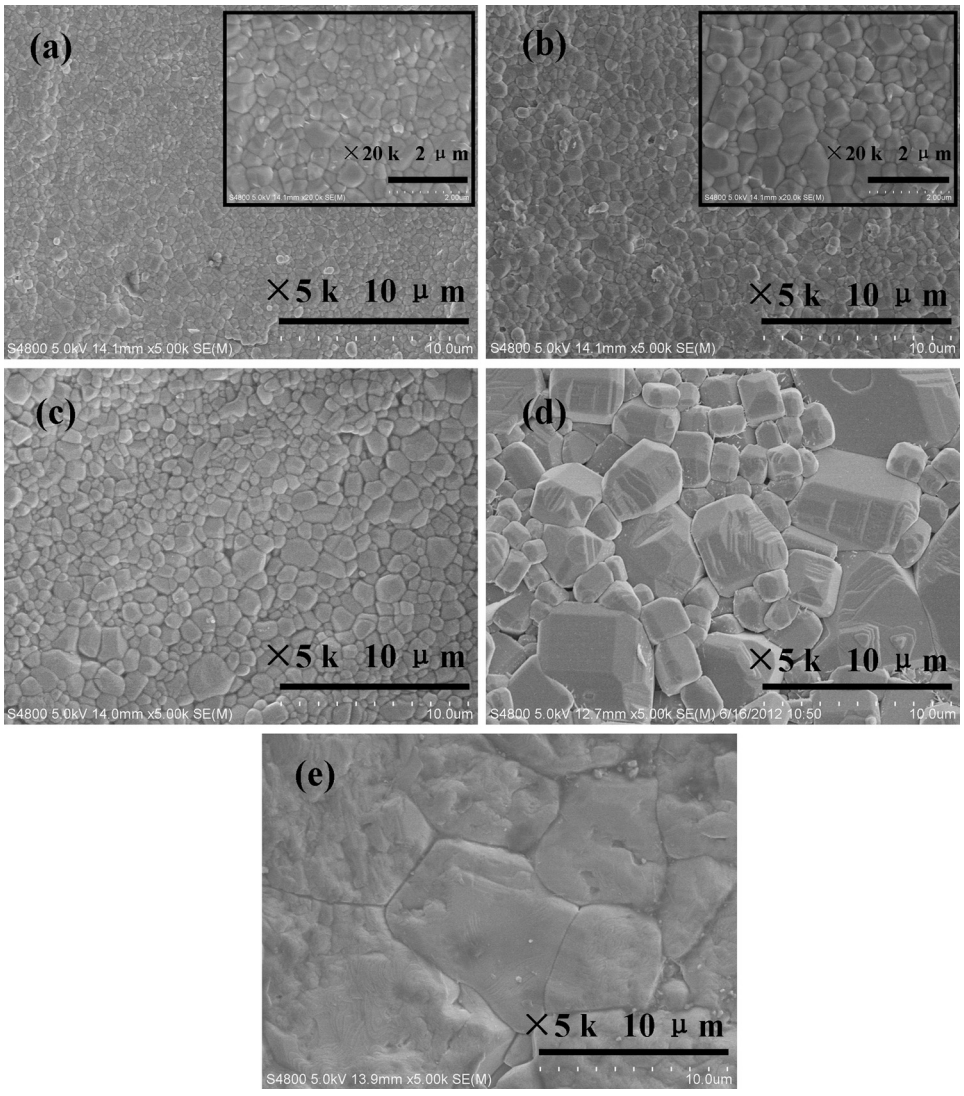

Fig. 2. SEM images on the surface of BST ceramics with different sintering temperatures as well as grain sizes: (a) 1260 °C–2 h, GS (grain size) = 0.5 μm; (b) 1280 °C–2 h, GS = 0.7 μm; (c) 1300 °C–2 h, GS = 1.2 μm; (d) 1350 °C–2 h, GS = 2.2 μm; and (e) 1400 °C–2 h, GS = 5.6 μm.

varying in the range of 0 kV/cm to 20 kV/cm. It was found that the dielectric constant increased to ~1180 gradually with increasing grain size in a certain range of 0.5–2.2 μm, as predicted by the "series and parallel combination" model.[6] However, the dielectric constant of BST ceramic with the grain size of 5.6 μm is lower than that of sample with grain size of 2.2 μm, which may due to the over-sintering at 1400 °C.

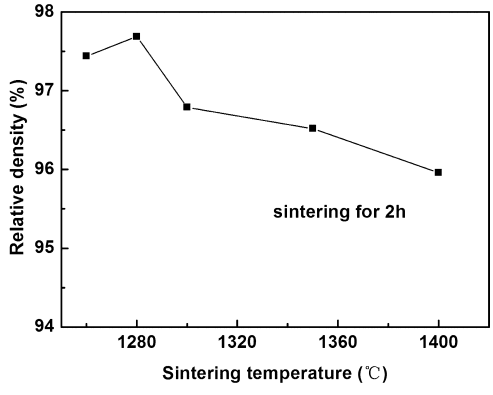

Fig. 3. Relative density of BST ceramics sintering at different temperatures.

For all samples, the dielectric constants tend to be reduced slightly with increasing bias electric field, showing weaker dielectric nonlinearity even in paraelectric phase. This can be explained by the Devonshire's phenomenological theory[20] where this phenomenon is attributed to the suppression of the anharmonic interaction of Ti^{4+} ions in Ti–O octahedrons.

To characterize the dielectric nonlinearity, the dielectric tunability k is defined at a specific dc bias electric field:

$$k = \frac{\varepsilon_{r(0)} - \varepsilon_{r(E)}}{\varepsilon_{r(0)}} \times 100\% \quad (2)$$

where $\varepsilon_{r(0)}$ and $\varepsilon_{r(E)}$ are the dielectric constants under zero bias field and applied bias field E, respectively.

As listed in Table 1, when the applied bias field is up to 20 kV/cm, compared with ferroelectric $BaTiO_3$,[21] the dielectric tunability of $(Ba_{0.4}Sr_{0.6})TiO_3$ is much lower, being <5% and the tunability is reduced gradually with decreasing grain sizes.

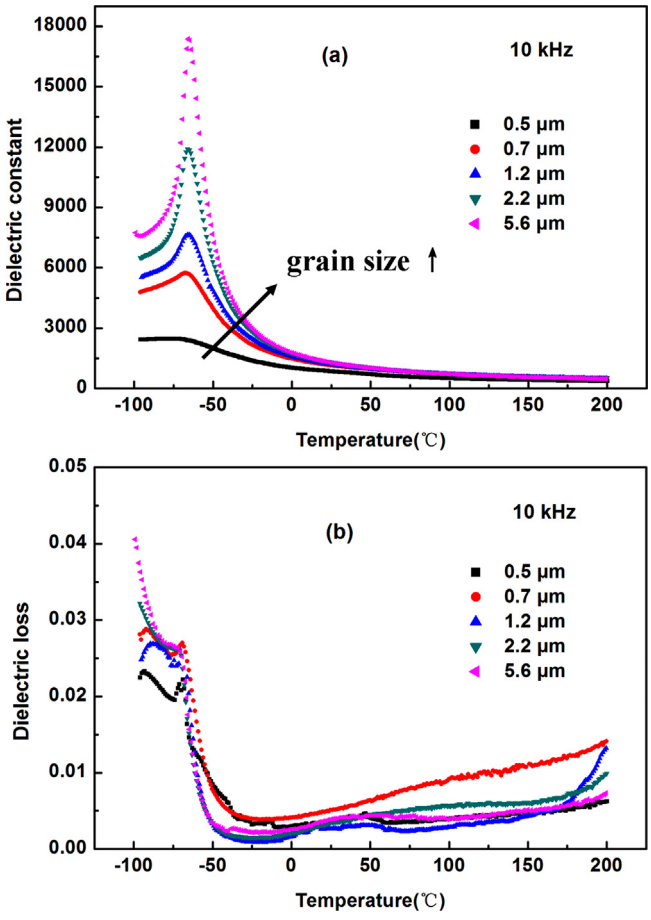

Fig. 4. Dielectric constant (a) and dielectric loss (b) versus temperature for $(Ba_{0.4}Sr_{0.6})TiO_3$ dense ceramics with different grain sizes at the frequency of 10 kHz.

Dielectric ceramics can be regarded as a composite including ferroelectric grain cores with high dielectric constant and insulated grain boundary layers with low dielectric constant. Under the bias field, the grain boundary remains linear and makes no contribution to the dc-tunability. As the grain size decreases, the volume fraction of the grain boundary (i.e. the grain boundary density) increases, thus the "dilution" effect on the dielectric nonlinearity becomes more evident, which can explain the depressed dielectric tunabilities with decreasing grain size.[22]

Table 1
Dielectric tunability and slope of fitting lines in Fig. 6 for BST ceramics with various grain sizes.

Samples	Grain size (μm)	Dielectric tunabilities (%)	Slopes of fitting lines $(kV/cm)^{-2}$
1#	0.5	1.14	0.99×10^{-2}
2#	0.7	1.27	1.01×10^{-2}
3#	1.2	3.83	2.93×10^{-2}
4#	2.2	4.28	3.38×10^{-2}
5#	5.6	5.85	4.69×10^{-2}

3.2.2. *Grain size effect on the nonlinearity mechanisms*

The nonlinear variation of ε_r for BST paraelectric ceramics under bias electric field could be fitted to the Johnson's phenomenological expression based on the Devonshire's phenomenological theory, as described by the following[23]:

$$\frac{\varepsilon_{r(E)}}{\varepsilon_{r(0)}} = \frac{1}{[1 + \alpha\varepsilon_{r(0)}^3 E^2]^{1/3}} \quad (3)$$

wherein α represents the anharmonic coefficient, corresponding to the levels of anharmonic interactions among Ti^{4+} ions.

The fitting results of the dielectric nonlinearity of BST ceramics with various grain sizes according to the Johnson's expression are shown in Fig. 6. The $(\varepsilon_{r(0)}/\varepsilon_{r(E)})^3$ vs. E^2 plots of the BST samples show linear behaviors, which are in good agreement with the Johnson's expression, indicating the dielectric nonlinearity of BST paraelectric ceramics is dominated by the suppression of the anharmonic interaction of Ti^{4+} ions according to the Devonshire's phenomenological theory. The fitting slopes (representing $\alpha\varepsilon_{r(0)}^3$ in Eq. (3)) were found to increase gradually with the grain size increasing, being consistent with the variation of the dielectric tunability, as listed in Table 1.

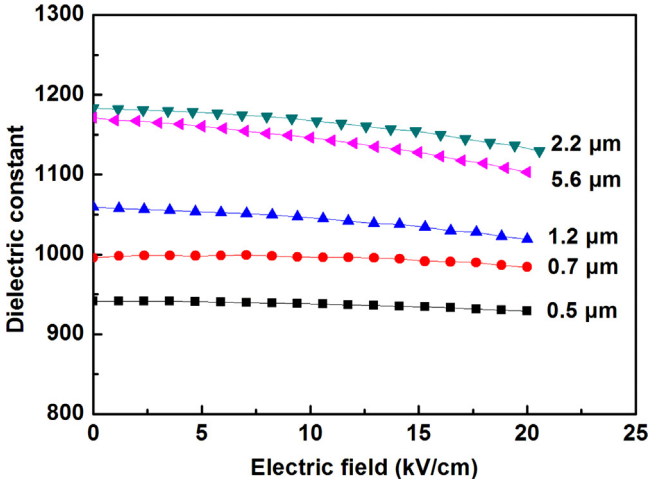

Fig. 5. The dielectric constant as a function of bias electric field for BST ceramics with different grain sizes.

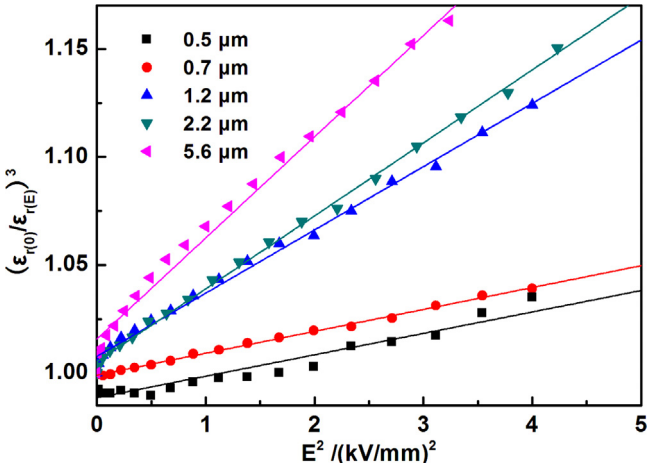

Fig. 6. The fitting results of dielectric nonlinearity of BST ceramics with various grain sizes according to Johnson formula.

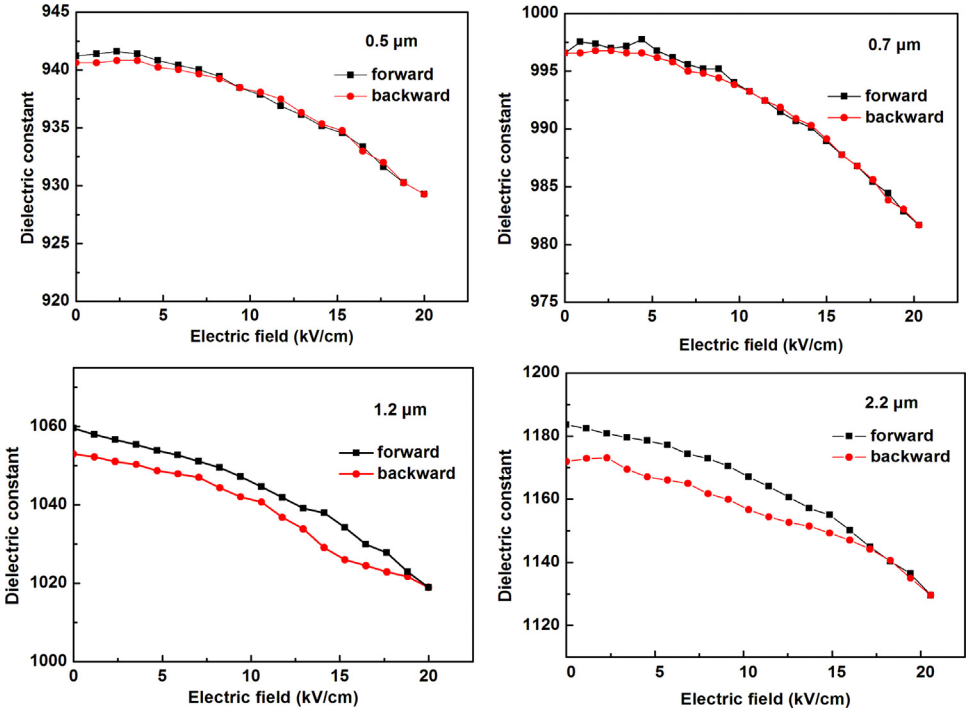

Fig. 7. Bias electric field circuits for BST ceramics with various grain sizes.

The ε_r vs. E circuits for field-increasing (the forward direction) and field-decreasing (the backward direction) of BST ceramics with various grain sizes are comparatively presented in Fig. 7. Generally, the dielectric constants in field-increasing curves are higher than that in field-decreasing curves due to the response of polar nano-regions (PNRs) under bias electric field.[24] During the field-increasing process, the polarization reorientation and arrangement of PNRs occurs, while the field-induced behavior is partially frozen under the field-decreasing conditions. As a result, the polarization contribution of PNRs to the dielectric constant is depressed and the deviation phenomenon occurs between the field-increasing and field-decreasing processes. Here, PNRs generally refer to nano-sized polar clusters and are strongly dependent on the grain sizes, which were observed in paraelectric BST induced by the local polar movement of Ti^{4+} ions.[25]

As shown in Fig. 7, the field-increasing curves were found to overlap with the field-decreasing curves for samples with smaller grain sizes of 0.5 μm and 0.7 μm. The deviation degree between the forward and backward directions was found to increase with increasing grain sizes, which was thought to be mainly induced by the variation of PNRs' polarization response under bias fields.

In order to characterize the polarization contribution of PNRs to paraelectric BST with different grain sizes, the dielectric constants under bias field were fitted to the multi-polarization mechanism model, which is derived from the Johnson's phenomenological expression,[26]

$$\varepsilon_{r(E)} = \frac{\varepsilon_{r(0)}}{[1+\alpha(\varepsilon_0\varepsilon_{r(0)})^3E^2]^{1/3}} + \sum\left(\frac{P_0x}{\varepsilon_0}\right)[\cosh(Ex)]^{-2} \quad (4)$$

in which $x = P_0V/k_BT$, P_0 and V are the polarization and equivalent volume for extrinsic polarization entities, which are proposed as PNRs. The first term of the equation, i.e. the Johnson's term, refers to the intrinsic polarization mechanism (the anharmonic interactions among Ti^{4+} ions). And the second term, i.e. the PNRs' term, represents the extrinsic contributions of PNRs.

Fig. 8 shows the fitting curves according to the multi-polarization mechanism model for the samples with different grain sizes. The fitting plots are generally coincide with the experimental data, where the polarization response of the intrinsic and extrinsic mechanisms could be separated. As shown in Fig. 8, PNRs' contributions to dielectric constant are relatively low compared with the intrinsic term. For ceramics with larger grains (1.2 μm and 2.2 μm), the sensitivity of PNRs to bias field increases significantly and their contributions to dielectric constant are minimized to zero and remain high stability with the bias field above 5 kV/cm.

The characteristic parameters of PNRs were obtained from the fitting results, as listed in Table 2, in which d is the equivalent size of PNRs, being equal to $V^{1/3}$ in Eq. (4). Of particular significance is that with increasing grain sizes, the polarization of PNRs tends to be reduced and their equivalent sizes increase gradually. For ceramics with grain size of 1.2 μm and 2.2 μm, the equivalent size of PNRs expands to 1.37 nm and 4.04 nm,

Table 2
Characteristics of polar nano-regions in BST ceramics with various grain sizes.

Grain sizes (μm)	0.5	0.7	1.2	2.2
P_0 (μC/cm^2)	6.28	1.54	0.075	0.041
d (nm)	0.19	0.30	1.37	4.04

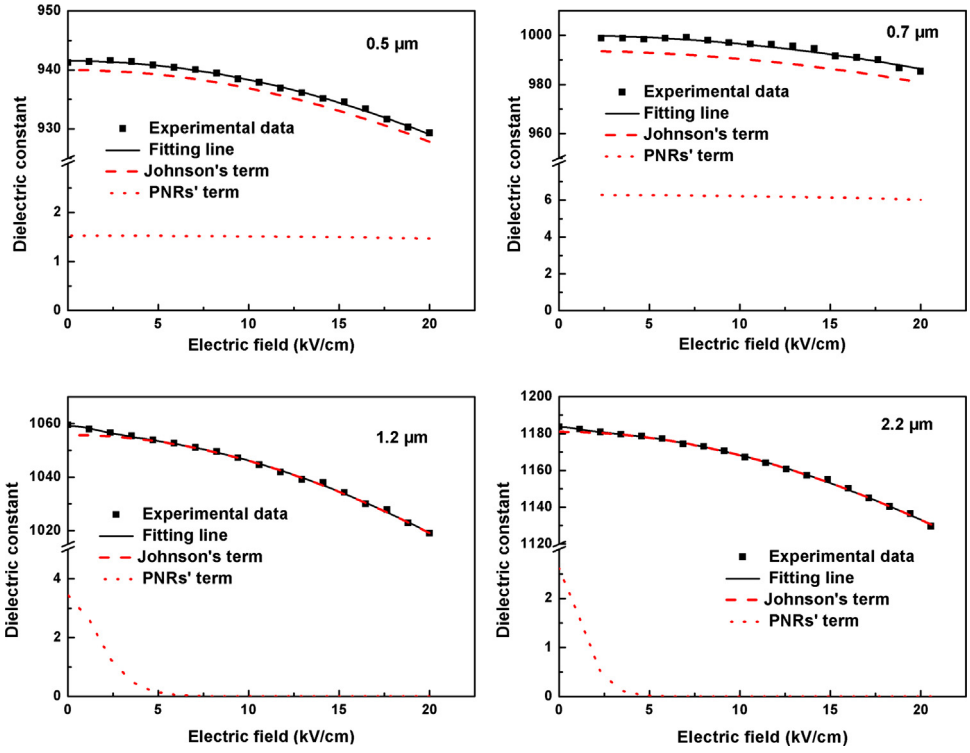

Fig. 8. Fitting curves according to the multi-polarization mechanism model of BST ceramics with various grain sizes.

respectively, revealing that the dielectric response of PNRs is dependent on the grain sizes.

3.3. Grain size effect on energy storage properties

P–E hysteresis loops of $(Ba_{0.4}Sr_{0.6})TiO_3$ with various grain sizes achieved at different applied electric fields prior to dielectric breakdown strength (maximum electric fields) are shown in Fig. 9. The hysteresis characteristic of the samples with various grain sizes is also dependent on the applied electric field, in addition to the materials properties. For sample with 0.5 μm grain size, the broadening of the hysteresis loop is mainly due to the mass accumulation of the space charge at the grain boundary interface under a higher electric field.[27] With the decrease of grain size, the dielectric breakdown strength increases, thus the applied electric field can be enhanced greatly, leading to the enhancement of space charge effect, accompanied by a higher leakage current, as demonstrated by the lossy *P–E* loop.[28] For samples with 2.2 μm and 5.6 μm grain sizes, on the contrary, slim hysteresis loops were obtained due to the lower applied fields.

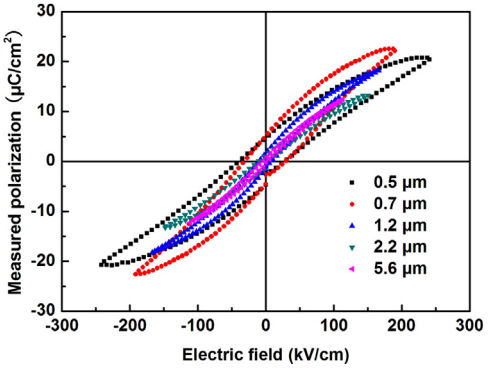

Fig. 9. The hysteresis loops of BST ceramics with various grain sizes.

The energy storage performance parameters of all samples can be evaluated from the hysteresis loops, as listed in Table 3. The energy density γ was calculated by integrating the area between the polarization axis and the discharge curve in the *P–E* hysteresis loop. With the decrease of grain size, the dielectric breakdown strength (E_b) improves obviously, accompanied by the increase of maximum polarization (P_{max}), which will favor a higher energy density. Sample 1# with the minimum grain size of 0.5 μm exhibits the maximum energy density, being on the order of 1.28 J/cm^3 due to its highest dielectric breakdown strength (243 kV/cm) and relatively high maximum polarization (20.6 μC/cm^2).

The significant improvement of E_b for samples with smaller grain size was considered to be associated with the increase of the grain boundary density. As discussed in Section 3.2.1, dielectric ceramics can be regarded as a composite including ferroelectric grain cores and insulated grain boundary layers. The volume fraction of the grains and grain boundaries changes with grain size variation, which plays an important role for the dielectric breakdown strength.

3.4. Grain size effect on complex impedance characteristics

To examine the variation tendency about the volume/size ratio of the grain-grain boundary quantitatively, complex impedance

Table 3
Energy storage properties of BST ceramics with various grain sizes.

Samples	Grain size (μm)	E_b (kV/cm)	Maximum polarization, P_{max} (μC/cm^2)	Energy density, γ (J/cm^3)
1#	0.5	243	20.6	1.28
2#	0.7	191	22.3	1.20
3#	1.2	167	18.3	1.11
4#	2.2	151	13.2	0.76
5#	5.6	114	12.5	0.60

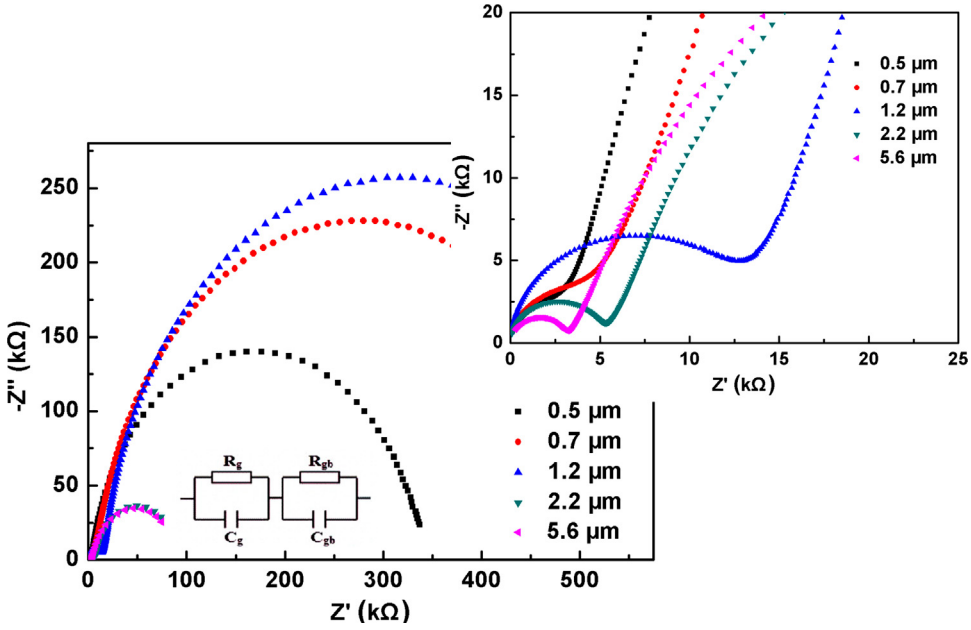

Fig. 10. Complex plane impedance plots of BST ceramics with various grain sizes at 420 °C. Inset 1: the enlarged scale of high frequency area. Inset 2: equivalent circuit proposed for electrical microstructure of BST ceramics.

spectroscopy was used to analyze the electrical microstructure of BST ceramics at the activation temperature of 420 °C and in the frequency range of 20 Hz–2 MHz. As shown in Fig. 10, two semicircular plots with different radii were observed in the complex impedance planes, in which the smaller-sized semicircle corresponds to the response from grain while the larger-scaled one represents the contributions from grain boundary, respectively.

The two semicircular arcs in the impedance spectrum can be simulated by a parallel *R*–*C* equivalent circuit,[29–31] as shown in the inset in Fig. 10. Based on the equivalent circuit, the resistances and capacitances of different electrical regions (grain and grain boundary) can be calculated by using the Z-View software. The calculated R_g, R_{gb}, C_g and C_{gb} values are given in Table 4. For all samples, the values of R_{gb} are considerably larger than R_g, indicating the better insulation performance of the grain boundaries. The electrical parameters of grain regions as well as grain boundaries were found to change significantly as a function of grain size. Due to the fact that the intrinsic electrical properties (such as the resistivity ρ and the dielectric constant) of the grains and the grain boundaries remain unchanged for BST with varying grain sizes, the changes of *R*, *C* values are mainly owing to the variation of the grain size and grain boundary density.

The contribution of the grain boundary density to the grain size effect can be analyzed by a double-layered dielectric

Table 4
Electrical parameters at 420 °C of different electrical regions for BST ceramics with various grain sizes.

Grain size (μm)	R_g (Ω)	R_{gb} (Ω)	R_g/R_{gb}	C_g (pF)	C_{gb} (pF)	C_{gb}/C_g
0.5	4206	304,860	0.01380	137.5	804	5.8516
0.7	6601	467,820	0.01411	136.3	1358	9.9633
1.2	14,498	464,510	0.03121	133.9	7736	57.7745
2.2	5753	69,737	0.08250	148.7	30,839	207.3907
5.6	3558	66,983	0.05318	97.0	21,196	218.5605

model[32] based on the R, C electrical parameters. The capacitances of the grains and grain boundaries can be described as:

$$C_g = \frac{\varepsilon_g \cdot A_g}{d_g} \quad (5)$$

$$C_{gb} = \frac{\varepsilon_{gb} \cdot A_{gb}}{d_{gb}} \quad (6)$$

where ε_g and ε_{gb}, A_g and A_{gb}, d_g and d_{gb} represent the dielectric constants, the contact areas, and the mean sizes of the grains and grain boundaries, respectively. In the double-layered dielectric model, it is considered that the grains and grain boundaries share nearly equal contact areas, i.e. $A_g = A_{gb}$. Hence, Eq. (5) and Eq. (6) can be simplified.

$$\frac{C_g}{C_{gb}} = \left(\frac{\varepsilon_g}{\varepsilon_{gb}}\right) \cdot \left(\frac{d_{gb}}{d_g}\right) \quad (7)$$

Similarly, for R_g and R_{gb} the formula can be expressed as:

$$\frac{R_g}{R_{gb}} = \left(\frac{\rho_g}{\rho_{gb}}\right) \cdot \left(\frac{d_g}{d_{gb}}\right) \quad (8)$$

With varying the grain sizes, the resistivity ρ and dielectric constant of the grains and grain boundaries remain unchanged, so do the $\varepsilon_g/\varepsilon_{gb}$ and ρ_g/ρ_{gb} terms. Therefore, it is reasonable that the volume fraction of the grains and grain boundaries (i.e. the variation of d_g/d_{gb}) with the change of grain sizes can be described by the C_{gb}/C_g and R_g/R_{gb} values. It can be seen from Table 4 that with increasing the grain size, the ratios of C_{gb}/C_g and R_g/R_{gb} increase gradually, corresponding to the increase of d_g/d_{gb}, confirming the increase of the volume fraction of ferroelectric grain cores as well as the decrease of insulated grain boundaries, as a function of increasing grain size. It is believed that the variation of the volume fraction of the grains and grain boundaries has an important impact on the grain size effect.

4. Conclusions

In summary, the variation of grain sizes has a significant impact on the energy storage properties of $Ba_{0.4}Sr_{0.6}TiO_3$ paraelectric ceramics. As the grain size reduced from 5.6 μm to 0.5 μm, a clear tendency toward a diffuse phase transition related to the effect of internal stress was observed. With decreasing grain sizes, the dielectric nonlinearity is depressed gradually, driven by the decreasing density of the ferroelectric grains, as well as the increasing of insulated grain boundaries. The grain size-dependent nonlinearity mechanisms (the intrinsic polarization and PNRs) were discussed. The weaker dielectric nonlinearity for $Ba_{0.4}Sr_{0.6}TiO_3$ ceramics can be explained by the Devonshire's phenomenological theory (from the viewpoint of intrinsic polarization), while the polarization behavior of PNRs is believed to make a unique contribution to the nonlinear characteristic of $Ba_{0.4}Sr_{0.6}TiO_3$ ceramics. Based on the multi-polarization mechanism model, it was found that with increasing grain size, the polarization of PNRs tends to be reduced and their equivalent sizes increase gradually. And the refinement of grains will benefit the energy density for BST. The grain boundary density was thought to play an important role on the improvement of dielectric breakdown strength, which was confirmed by the complex impedance spectroscopy analysis based on a double-layered dielectric model.

Conflicts of interest

The authors have no conflicts of interest to declare.

Acknowledgements

This work was supported by the Key Program of Natural Science Foundation of China (No. 50932004), the International Science and Technology Cooperation Program of China (2011DFA52680), the Natural Science Foundation of China (No. 51102189, No. 51372191), the Program for New Century Excellent Talents in University (No. NCET-11-0685), and the Self-determined and Innovative Research Funds of WUT (No. 135101018).

References

1. Ricketts BW, Triani G, Hilton AD. Dielectric energy storage densities in $Ba_{1-x}Sr_xTi_{1-y}Zr_yO_3$ ceramics. *J Mater Sci – Mater Electron* 2000;**11**:513–7.
2. Zhou L, Vilarinho PM, Baptista JL. Dependence of the structural and dielectric properties of $Ba_{1-x}Sr_xTiO_3$ ceramic solid solutions on raw material processing. *J Eur Ceram Soc* 1999;**19**:2015–20.
3. Kniekamp H, Heywang W. Depolarization effects in polycrystalline $BaTiO_3$. *Z Angew Phys* 1954;**6**:385–90.
4. Buessem WR, Cross LE, Goswami AK. Phenomenological theory of high permittivity in fine-grained barium titanate. *J Am Ceram Soc* 1966;**49**:33–6.
5. Arlt G, Hennings D, De With G. Dielectric properties of fine-grained barium titanate ceramics. *J Appl Phys* 1985;**58**:1619–25.
6. Shaikh AS, Vest RW, Vest GM. Dielectric properties of ultrafine grained $BaTiO_3$. *IEEE Trans Ultrason Ferroelectr Freq Control* 1989;**36**:407–12.
7. Zhai JW, Chen H, Chou CC, Raevskaya SI, Prosandeev SA, Raevski IP. Peculiarities of temperature and field dependence of tunability in $Ba_{0.6}Sr_{0.4}TiO_3$ceramics with differing grain sizes. *J Alloys Compd* 2011;**509**:6113–6.
8. Young A, Hilmas G, Zhang SC, Schwartz RW. Effect of liquid-phase sintering on the breakdown strength of barium titanate. *J Am Ceram Soc* 2007;**90**:1504–10.
9. Curecheriu L, Buscaglia MT, Buscaglia V, Zhao Z, Mitoseriu L. Grain size effect on the nonlinear dielectric properties of barium titanate ceramics. *Appl Phys Lett* 2010;**97**:242909.
10. Cao W, Randall C. Grain size and domain size relations in bulk ceramic ferroelectric materials. *J Phys Chem Solids* 1996;**57**:1499–505.
11. Kinoshita K, Yamaji A. Grain size effects on dielectric properties in barium titanate ceramics. *J Appl Phys* 1976;**47**:371–3.
12. Hilton AD, Ricketts BW. Dielectric properties of $Ba_{1-x}Sr_xTiO_3$ ceramics. *J Phys D: Appl Phys* 1996;**29**:1321–5.
13. Zhang QM, Wang L, Luo J, Tang Q, Du J. $Ba_{0.4}Sr_{0.6}TiO_3$/MgO composites with enhanced energy storage density and low dielectric loss for solid-state pulse-forming line. *Int J Appl Ceram Technol* 2010;**7**:E124–8.
14. Love GR. Energy storage in ceramic dielectrics. *J Am Ceram Soc* 1990;**73**:323–8.
15. Fletcher NH, Hilton AD, Ricketts BW. Optimization of energy storage density in ceramic capacitors. *J Phys D: Appl Phys* 1996;**29**:253–8.
16. Fang TT, Hsieh HL, Vest GM. Effects of pore morphology and grain size on the dielectric properties and tetragonal-cubic phase transition of high-purity $BaTiO_3$. *J Am Ceram Soc* 1993;**76**:1205–11.

17. Tang XG, Chan HLW. Effect of grain size on the electric properties of (Ba,Ca)(Zr·Ti)O_3 relaxor ferroelectric ceramics. *J Appl Phys* 2005;**97**(3):034109.
18. Frey MH, Payne DA. Grain-size effect on structure and phase transformations for barium titanate. *Phys Rev B* 1996;**54**(5):3158–68.
19. Liu P, Ma JL, Meng L, Zhang HW, et al. Preparation and dielectric properties of BST-Mg_2TiO_4 composite ceramics. *Mater Chem Phys* 2009;**114**(2–3):624–8.
20. Liang RH, Dong XL, Chen Y, Cao F, Wang YLU. Mechanism of nonlinear dielectric constant of $BaTiO_3$-based ceramics under high DC electric field. *Acta Phys Sin* 2005;**54**(10):4914–9.
21. Tagantsev AK, Sherman VO, Astafiev KF, Venkatesh J, Setter N. Ferroelectric materials for microwave tunable applications. *J Electroceram* 2003;**11**:5–66.
22. Curecheriu L, Balmus SB, Buscaglia V, Mitoseriu L, et al. Grain size-dependent properties of dense nanocrystalline barium titanate ceramics. *J Am Ceram Soc* 2012;**95**(12):3912–21.
23. Xu Q, Zhang XF, Chen W, Kim BH, et al. Effect of MgO on structure and nonlinear dielectric properties of $Ba_{0.6}Sr_{0.4}TiO_3$/MgO composite ceramics prepared from superfine powders. *J Alloys Compd* 2009;**488**(1):448–53.
24. Xu Q, Zhang XF, Chen W, Liu HX, Kim BH, et al. Sinterability and nonlinear dielectric properties of $Ba_{0.6}Sr_{0.4}TiO_3$ derived from a citrate method. *J Alloys Compd* 2009;**485**(1–2):L16–20.
25. Ding YP, Meng ZY. The ordered micro-domain in $Ba_{1-x}Sr_xTiO_3$ thin films and its effect on phase transition. *J Mater Sci Lett* 2000;**19**:163–5.
26. Ang C, Yu Z. DC electric-field dependence of the dielectric constant in polar dielectrics: multi-polarization mechanism model. *Phys Rev B* 2004;**69**:174109.
27. Pontes FM, Leite ER, Longo E, Varela JA, Araujo EB, Eiras JA. Effects of the postannealing atmosphere on the dielectric properties of (Ba·Sr)TiO_3 capacitors: evidence of an interfacial space charge layer. *Appl Phys Lett* 2000;**76**(17):2433–5.
28. Jin L, Li F, Zhang SJ. Decoding the fingerprint of ferroelectric loops: comprehension of the material properties. *J Am Ceram Soc* 2014;**97**:1–27.
29. Ham YS, Koh JH. Impedance spectroscopy of Li_2CO_3 doped (Ba·Sr)TiO_3ceramic. *Solid State Sci* 2013;**16**:53–6.
30. Barick BK, Choudhary RNP, Pradhan DK. Dielectric and impedance spectroscopy of zirconium modified ($Na_{0.5}Bi_{0.5}$)TiO_3 ceramics. *Ceram Int* 2013;**39**:5695–704.
31. Wang ZJ, Cao MH, Yao ZH, Hao H, Liu HX, Yu ZY, Song Z. Effects of Sr/Ti ratio on the microstructure and energy storage properties of nonstoichiometric $SrTiO_3$ ceramics. *Ceram Int* 2014;**40**(1):929–33.
32. Yamamoto T, Takao S. Complex impedance analysis of Nb-doped ($Ba_{0.6}Sr_{0.4}$)TiO_3 PTC (positive temperature coefficient) thermistors. *Jpn J Appl Phys* 1992;**31**:3120–3.